

A dilute gold nanoparticles suspension as SAXS standard for absolute scale using an extended Guinier approximation

Ahmed S. A. Mohammed^{a,b,c}, Agnese Carino^d, Andrea Testino^d, Mohamed Reza Andalibi^d, Antonio Cervellino^{a,*}

^a Paul Scherrer Institute (PSI), Swiss Light Source (SLS), CH-5232 Villigen PSI, Switzerland

^b Physik-Institut der Universität Zürich, Winterthurerstrasse 190, CH-8057 Zürich, Switzerland

^c Physics Department, Faculty of Science, Fayoum University, 63514 Fayoum, Egypt

^d Paul Scherrer Institute (PSI), ENE, CH-5232 Villigen PSI, Switzerland

* *Corresponding author. Email: antonio.cervellino@psi.ch*

October 5, 2018

Abstract

In this article, a practical procedure for absolute intensity calibration for SAXS studies on liquid microjets is established, using a gold nanoparticle suspension as standard so that the intercept at $Q = 0$ of the SAXS scattering curve would provide a scaling reference. In order to get the most precise extrapolation at $Q = 0$, we used an extension to the Guinier approximation, with a second-order term in the fit that adapts to a larger Q -range.

1 Introduction

We were conducting a number of SAXS experiments on liquid jets requiring an absolute scale determination in order to estimate concentrations of very dilute samples in a dynamical state, whereas offline measurements could not yield the desired results. Moreover,

experiments were performed on a beamline that is not a dedicated SAXS instrument, where the accent is on flexibility of operation. Therefore instrument precalibration is excluded as too costly in terms of time and resources. Instead, we use SAXS standard of which everything is known and from which a predictable SAXS signal could be obtained in exactly the same experimental configuration, in order to derive the absolute scale constant from the extrapolation of the SAXS intensity to $Q \rightarrow 0$. Such a suitable standard was identified as a dilute suspension of known concentration (200 mg/L) of practically monodisperse oleate-capped Au nanoparticles, whose diameter was estimated to be 18 nm. The extrapolation to $Q \rightarrow 0$ was achieved using an extended Guinier method. In fact, in order to use an extended data range, the classical Guinier approximation was extended to one more term (*i.e.*, to the fourth order in Q).

2 Liquid microjet setup

A free liquid jet setup was developed to collect *in-situ* synchrotron small and wide angle X-ray scattering data (Mohammed *et al.* (2017)). Among different applications, this approach enables the study of the early stage of solids formation (nucleation). Such a mechanism is delicate and it is prone to be influenced by many factors (Carino *et al.* (2017); Marmioli *et al.* (2009)); in this fields, *in-situ* techniques are well-established and are able to provide reliable experimental results (Haberkorn *et al.* (2003)). A successful SAXS measurements setup was demonstrated by Schmidt and coworkers (Schmidt *et al.* (2010)) for ZnS precipitation. Here the aim is to study by *in-situ* SAXS measurements very diluted inorganic systems containing entities with an electron density slightly higher than that of the solvent. Our study was specifically designed to investigate the biominerals formation pathway, such as calcium carbonate and calcium phosphate, under controlled temperature, pH, and saturation conditions. The pulsation-free micrometric-size horizontal reacting liquid jet setup is composed by four HPLC pumps (each of them equipped with a pulsation damper system and a high precision Coriolis mass flowmeter), a micromixing system, a delay loop, and a catcher. The micromixer manifolds is equipped with 5 inputs and

one output. Four inputs are connected to the solutions contributing to the precipitation reaction whereas the fifth input was used for cleaning purposes and connected to an additional pump delivering 10 wt.% acetic acid. A delay loop (which consists of a teflon tube of a certain length and internal diameter) can be connected the micromixer output. This tube determines a delay time between the mixing point and the measuring point, where the free liquid jet is interrogated by the X-ray beam. A double-walled water-jacketed tubing system is used to thermostat the delay tube and the chemical delivery lines before the mixing point. A nozzle of different materials and sizes may be connected after the delay loop and used to generate the liquid jet. In this study, a stainless steel capillary with internal diameter of 250 μm and an overall flow rate of 8 ml min^{-1} was used. The main advantage of this approach is that the solid formation mechanisms can be followed while the liquid jet is continuously renovated, at a defined timeframe after the mixing point, therefore in static conditions with respect to the entities development, produced by the reaction, and with negligible perturbations of jet probed by the beam (negligible beam damage). Since the amount and electron density of the matter of interest is very low, an accurate experimental data collection needs to be carried out and data accumulated for a relatively long time at each experimental condition (static mode). Moreover, the absolute scale constant need to be evaluated. To this end, a well characterized diluted standard solution containing gold nanoparticles was used applying exactly the same experimental configuration of the precipitation experiments.

3 Standard preparation and characterization

The gold nanoparticle (GNP) suspension was synthesised using the citrate route, also called Turkevich method (*i.e.*, by reducing the tetrachloroauric acid (TCAA) precursors with trisodium citrate (Na_3cit) in water). The preparation was done using a segmented flow tubular reactor, SFTR (Jongen *et al.* (2003); Donnet *et al.* (2000); Aimable *et al.* (2011)). The SFTR allows monitoring accurately the ratio of the chemicals, the temperature, and the aging time. The segmentation is obtained using a secondary immiscible fluid

which also prevents fouling. The precursor solutions are mixed at room temperature and segmented into the tubular reactor as a sequence of droplets in which the reaction occurs triggered by the fast temperature rising of the tubular reactor. The obtained nanoparticle size distribution is narrow and reproducible. This reactor consents a continuous production up to 5 g of solid per day. The conditions used to prepare the GNP suspension were similar to the ones reported in a previous work (Carino *et al.* (2016)). The synthesis was done at 95 °C using a Na₃Cit to TCAA molar ratio equal to 7.9, an ageing time of 5 min, and the chemicals flow rate was 1 L h⁻¹. The final GNP concentration was of about 0.2 g L⁻¹ (measured by ICP-MS). The suspension presented a monomodal distribution of GNP with an average number diameter of 18 nm and a standard deviation < 8 % (measured by TEM imaging and dynamic light scattering).

4 Data collection

Synchrotron Small-Angle X-rays Scattering (SAXS) measurements were carried out at the Material Science beamline (X04SA–MS) of the Swiss Light Source (SLS) at PSI (Willmott *et al.* (2013)). This synchrotron station is built mainly for WAXS powder diffraction measurements but it also has some SAXS capabilities. The liquid jet, horizontal and orthogonal to the X-ray beam, was mounted on a double micrometric translation stage and optically centered with respect to the diffractometer circle by a high-resolution camera. The X-ray beam was set at 9.5 keV (corresponding to a wavelength $\lambda = 1.305\text{\AA}$) where the X-ray flux is maximal. Data were collected with the Mythen II detector system (Bergamaschi *et al.* (2010)), that with its 0.0036 *deg* step, has a sufficient resolution for SAXS on this system with a minimum accessible 2θ scattering angle of $\approx 0.18\text{ deg}$, corresponding to a minimum accessible momentum transfer of $Q = 4\pi \sin(\theta)/\lambda = 0.015\text{ \AA}^{-1}$. Scattering patterns were collected with reasonable acquisition times (20 min). Before the analysis, the experimental data were processed, corrected and rebinned to an uniform step Q grid, each data point being a triple Q -intensity-standard deviation.

4.1 Extended Guinier approximation

The Guinier approximation is a universal method (Guinier *et al.* (1955)) to derive some fundamental parameters from SAXS data exploiting some universal behaviour for $Q \rightarrow 0$ of the scattered intensity for diluted systems. If $I(Q)$ is the sample's scattered intensity, already subtracted of background terms and corrected for all instrumental aberrations, the Guinier approximation

$$I(Q) \approx A_0 e^{-bQ^2}$$

where $A_0 = I(Q = 0)$ and $b = R_g^2/3$ is related to the sample (appropriately averaged) gyration radius (see Sec. A.1, Eq. 7). This form is valid because $I(Q)$ is a smooth positive even function with a maximum at $Q = 0$ and monotonically decreasing for sufficiently small Q . It is usually recast as its MacLaurin expansion

$$\log(I(Q)) \approx \log(A_0) - bQ^2$$

A line fit of $\log(I(Q))$ *vs.* Q^2 yields then easily the values of A_0 and b . The range of validity of this approximation is however restricted to about

$$Q < \frac{\pi}{D}$$

where D is the scattering particle's diameter (in the case of a sphere).

A straightforward extension of this approximation is surely possible, whereas we suppose that $I(Q)$ at small Q can be described in the form

$$I(Q) \approx e^{a-bQ^2+cQ^4} \tag{1}$$

that is, with a further quartic term in the exponent. Again we do the Mac Laurin expansion

$$\log(I(Q)) \approx \log(A_0) - bQ^2 + cQ^4, \quad c \equiv C + \frac{b^2}{2} \tag{2}$$

where a second order polynomial in Q^2 replaces the straight line. A more technical

derivation is given in Appendix A.

4.2 Determination of the scale factor

We employ a water suspension of spherical Au nanoparticles of known concentration (200 mg/l) and known, practically unimodal size (18-19 nm) as standard to determine the absolute scale factor k . Such a suspension can be measured with the liquid jet with exactly the same setup as the investigated samples in this project. In fact, the observed intensity per unit time (after subtracting the background, including that of the liquid, measured separately) is

$$I(Q) = kN(\Delta\rho)^2V_p^2 \left(3 \frac{\sin(QR) - QR \cos(QR)}{(QR)^3} \right)^2 \quad (3)$$

where k is a constant pertaining to the experimental setup, N is the number of illuminated particles, $\Delta\rho$ is the particles' scattering contrast (the difference in scattering length density with respect to the average; hereafter we use electron units, where the classical electron radius $r_e = 1$, so $\Delta\rho$ has units of an inverse volume), V_p is the particle volume and the term within brackets is the analytical expression of the scattered intensity of a sphere.

The SAXS patterns were analyzed using the extended Guinier approximation of Eq. 2, discussed in Sec. 4.1. The parabolic fit is shown in Fig. 1. As our Q -range is contains relatively few points within the strict limits of validity of the standard Guinier approximation, the quadratic term in the fit allowed us to include an about three times wider Q -range, up to about $Q \approx 6/D$. The significance of the second order term is immaterial within the scope of this paper. Surely it helps gaining a more precise estimate of the other two parameters, especially A_0 . The extended Guinier fit yielded a gyration radius of 7.8799 ± 0.0116 nm corresponding - in the case of perfectly monodisperse spherical particles - to a particle diameter of 20.35 ± 0.03 nm, consistent (within the limits of the assumptions above) with an estimated diameter of 18 nm. More importantly, the

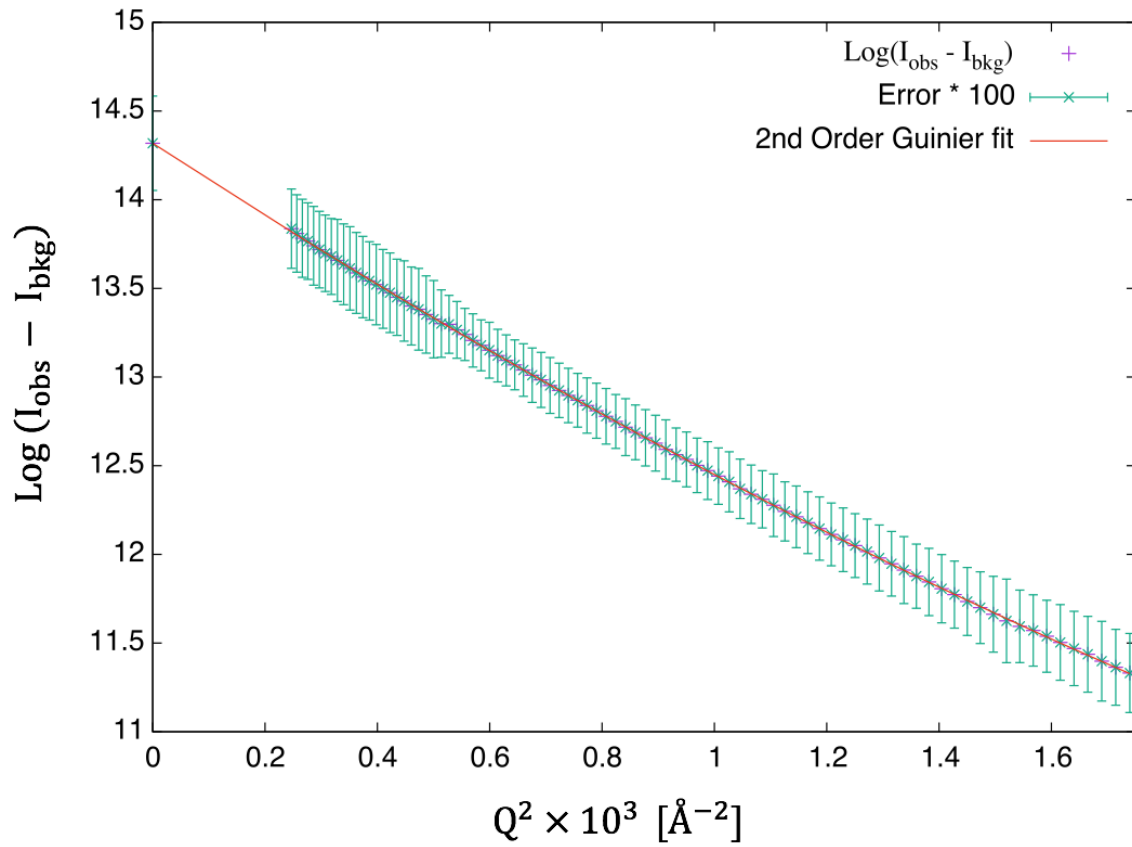


Figure 1: Guinier fit with second-order term added in order to exploit a larger Q -range and obtain a good estimate of the intercept, as needed for the absolute scale factor estimation.

extrapolated forward intensity was found to be

$$A_0 = I(Q = 0) = 1.6534 \times 10^6 \pm 4.4 \times 10^{-3} \text{ counts per second}$$

The average electron density of the suspension can be approximated with that of pure water, given the low concentration. For the Au NPs the density of bulk gold will be used. Therefore, evaluating the electron densities yields $\rho_{\text{H}_2\text{O}} = 3.34572 \times 10^{23} \text{ cm}^{-3}$; $\rho_{\text{Au}} = 4.66101 \times 10^{24} \text{ cm}^{-3}$; $\Delta\rho = 4.32644 \times 10^{24} \text{ cm}^{-3}$ From the given concentration and the Guinier diameter, we can assess that the number of Au NPs per cubic cm^3 is $n = 2.3499 \times 10^{12} \text{ cm}^{-3}$ and as the illuminated liquid volume was calculated as $V = 1.96350 \times 10^{-4} \text{ cm}^3$ so we have a total of $N = nV = 4.614 \times 10^8$ illuminated NPs. The particle volume, from the estimated diameter of 20.346 nm, results to $V_p = 4.4098 \times 10^{-18} \text{ cm}^3$ At $Q = 0$, the term in brackets in equation 3 is 1, so we can now solve for the sought-after scale factor:

$$k = \frac{I(Q = 0)}{N(\Delta\rho)^2 V_p^2} = 1.0114 \times 10^{-17} \quad (4)$$

5 Conclusions

We have demonstrated an external standard method to evaluate the scale factor for absolute intensity in SAXS experiments involving a liquid jet containing nanoparticles. The standard for liquid jet-type experiments is a suspension of as much as possible monodisperse nanoparticles of known concentration, high contrast, spherical shape and a known size that is similar to that of the samples under investigation. An extended Guinier approximation has been introduced, in order to improve the fit and consequently to achieve a more precise estimate of the extrapolated intensity at $Q = 0$. The method is simple, cheap, rapid (as it requires only one additional scattering measurement) and easily applicable to any beamline or instrument where a liquid jet device is installed. This also removes the need to perform a much tougher calibration of the instrument when absolute scale data are desired, while preserving also the same flexibility of operation of

relative-scale instruments.

A Theory

The Guinier approximation can be more rigorously derived by using its universal expression given by the Debye scattering equation (free from interparticle interference effects, as appropriate for diluted systems). The Debye scattering equation (Debye (1915)) yields the orientation averaged differential cross section directly from the atomic scattering density. Note that as we anyway consider a very small Q range, we can assume that atomic scattering factors (scattering lengths) are constant and independent from Q also for X-rays, slightly simplifying the discussion.

The atomic scattering density of a particle containing N_a atoms that have scattering lengths (or scattering factors) b_j and are located at positions \mathbf{r}_j for $j = 1, \dots, N_a$ is represented as

$$\rho(\mathbf{r}) = \sum_{j=1}^{N_a} b_j \delta(\mathbf{r} - \mathbf{r}_j)$$

As the origin is arbitrary, we refer the atomic coordinates to the scattering center of mass, so that

$$\sum_{j=1}^{N_a} b_j \mathbf{r}_j \equiv 0 \tag{5}$$

We also call B_1 , B_2 the sum of scattering lengths and that of their squares:

$$B_1 \equiv \sum_{j=1}^{N_a} b_j; \quad B_2 \equiv \sum_{j=1}^{N_a} b_j^2 \tag{6}$$

A.1 Radial moments

The radial moments of a density are defined as

$$M_n = \frac{\int d^3\mathbf{r} \rho(\mathbf{r}) \mathbf{r}^n}{\int d^3\mathbf{r} \rho(\mathbf{r})}$$

where $\underline{\mathbf{r}}^{2m} \equiv (\underline{\mathbf{r}} \cdot \underline{\mathbf{r}})^m = r^{2m}$ for even n , $\underline{\mathbf{r}}^{2m+1} \equiv (\underline{\mathbf{r}} \cdot \underline{\mathbf{r}})^m \underline{\mathbf{r}} = r^{2m} \underline{\mathbf{r}}$ for odd n . Thanks to Eq. (5), the odd moments are all zero. We can now evaluate the even radial moments of this density:

$$M_{2n} = \frac{\int d^3 \underline{\mathbf{r}} \rho(\underline{\mathbf{r}}) r^{2n}}{\int d^3 \underline{\mathbf{r}} \rho(\underline{\mathbf{r}})} = \frac{1}{B_1} \sum_{j=1}^{N_a} b_j r_j^{2n} \quad (7)$$

In particular, M_2 is called the squared gyration radius

$$r_g^2 = M_2$$

The differential cross section as a function of the transferred momentum $\underline{\mathbf{Q}}$ (where $Q = 4\pi \sin \theta / \lambda$) is

$$I(\underline{\mathbf{Q}}) = \sum_{j,k=1}^{N_a} b_j b_k e^{i\underline{\mathbf{Q}} \cdot (\underline{\mathbf{r}}_j - \underline{\mathbf{r}}_k)} = B_2 + 2 \sum_{j>k=1}^{N_a} b_j b_k e^{i\underline{\mathbf{Q}} \cdot (\underline{\mathbf{r}}_j - \underline{\mathbf{r}}_k)} \quad (8)$$

Here in evidence (first term on the RHS) is the self-scattering B_2 (*cf.* Eq. 6). Making the orientation average over all possible $\underline{\mathbf{Q}}$ directions, we obtain the Debye scattering equation (with $\text{sinc}(x) \equiv \sin(x)/x$)

$$I(Q) = \sum_{j,k=1}^{N_a} b_j b_k \text{sinc}(Q |\underline{\mathbf{r}}_j - \underline{\mathbf{r}}_k|) = B_2 + 2 \sum_{j>k=1}^{N_a} b_j b_k \text{sinc}(Q d_{jk}) \quad (9)$$

where $d_{jk} \equiv |\underline{\mathbf{r}}_j - \underline{\mathbf{r}}_k|$. Now we consider only the structural term $I_s(Q) = I(Q) - B_2$. The pair correlation function, that is the sinc transform of $I_s(Q)$, is

$$f_s(r) = \int_0^{+\infty} 4\pi Q^2 dQ \text{sinc}(Qr) I_s(Q) = 2 \sum_{j>k=1}^{N_a} \frac{b_j b_k}{4\pi r d_{jk}} \delta(r - d_{jk})$$

We want to calculate

$$Z_2 = \int_0^{+\infty} 4\pi r^2 dr f_s(r) r^2 = 2 \sum_{j>k=1}^{N_a} b_j b_k d_{jk}^2 = \sum_{j,k=1}^{N_a} b_j b_k (r_j^2 + r_k^2 - 2\underline{\mathbf{r}}_j \cdot \underline{\mathbf{r}}_k) \quad (10)$$

where we have expanded the distance squared and re-added the diagonal terms as they are 0 anyway. Now we split the sum in 3 parts, each with one of the terms in brackets, and reorder:

$$\sum_{j,k=1}^{N_a} b_j b_k r_j^2 = \sum_{j,k=1}^{N_a} b_j b_k r_k^2 = B_1 \sum_{j=1}^{N_a} b_j r_j^2 = B_1^2 r_g^2 \quad (11)$$

$$-2 \sum_{j,k=1}^{N_a} b_j b_k \underline{\mathbf{r}}_j \cdot \underline{\mathbf{r}}_k = -2 \left(\sum_{k=1}^{N_a} b_k \underline{\mathbf{r}}_k \right) \cdot \left(\sum_{j=1}^{N_a} b_j \underline{\mathbf{r}}_j \right) = 0 \quad (12)$$

the last is a consequence of Eq. (5). Therefore $Z_2 = 2B_1^2 r_g^2$ and the gyration radius can be evaluated also directly from the pair correlation function, as

$$r_g^2 = \frac{Z_2}{2B_1^2}$$

using Eqs. (6,10).

The Guinier approximation can be now derived from Eq. (9). There we can expand $I(Q)$ for small Q in a Mac Laurin series:

$$I(Q) = \sum_{j,k=1}^{N_a} b_j b_k - \frac{Q^2}{6} \sum_{j,k=1}^{N_a} b_j b_k d_{jk}^2 + \frac{Q^4}{120} \sum_{j,k=1}^{N_a} b_j b_k d_{jk}^4 - \frac{Q^6}{5040} \sum_{j,k=1}^{N_a} b_j b_k d_{jk}^6 + \dots \quad (13)$$

Being $I(Q)$ a positive, continuous and even function, its logarithm can also be expanded in a MacLaurin series that will contain only even powers of Q . Therefore, if we equate

$$I(Q) = \exp \left(\sum_{m=1}^{+\infty} a_m Q^{2m} \right)$$

and expand it also in a MacLaurin series, we can then equate coefficients of equal powers

of Q . The first 3 terms (up to Q^4) yield three equations:

$$e^{a_0} = \sum_{j,k=1}^{N_a} b_j b_k = B_1^2 \quad (14)$$

$$a_1 e^{a_0} = -\frac{1}{6} \sum_{j,k=1}^{N_a} b_j b_k d_{jk}^2 = -\frac{1}{3} B_1^2 r_g^2 \quad (15)$$

$$\frac{1}{2}(a_1^2 + 2a_2) e^{a_0} = \frac{1}{120} \sum_{j,k=1}^{N_a} b_j b_k d_{jk}^4 \quad (16)$$

and so on. Solving the first 2 equations, we have

$$a_0 = 2 \log(B_1); \quad a_1 = -\frac{1}{3} B_1^2 r_g^2$$

as in the classical Guinier approximation. From the third equation one could derive an expression for a higher radial moments M_4 .

References

- A. S. Mohammed, A. Cervellino, A. Testino, and A. Carino, *Acta Crystallogr. A Suppl.* **70**, C315 (2017).
- A. Carino, A. Testino, M. R. Andalibi, F. Pilger, P. Bowen, and C. Ludwig, *Crystal Growth & Design* **17**, 2006 (2017).
- B. Marmiroli, G. Greci, F. Cacho-Nerin, B. Sartori, E. Ferrari, P. Laggner, L. Businaro, and H. Amenitsch, *Lab on a Chip* **9**, 2063 (2009).
- H. Haberkorn, D. Franke, T. Frechen, W. Goesele, and J. Rieger, *Journal of Colloid and Interface Science* **259**, 112 (2003).
- W. Schmidt, P. Bussian, M. Lindn, H. Amenitsch, P. Agren, M. Tiemann, and F. Sch?th, *Journal of the American Chemical Society* **132**, 6822 (2010).
- N. Jongen, M. Donnet, P. Bowen, J. Lemaître, H. Hofmann, R. Schenk, C. Hofmann, M. Aoun-Habbache, S. Guillemet-Fritsch, J. Sarrias, *et al.*, *Chemical Engi-*

- neering & Technology: Industrial Chemistry-Plant Equipment-Process Engineering-Biotechnology **26**, 303 (2003).
- M. Donnet, N. Jongen, J. Lemaitre, and P. Bowen, Journal of Materials Science Letters **19**, 749 (2000).
- A. Aimable, N. Jongen, A. Testino, M. Donnet, J. Lemaître, H. Hofmann, and P. Bowen, Chemical Engineering & Technology **34**, 344 (2011).
- A. Carino, A. Walter, A. Testino, and H. Hofmann, CHIMIA International Journal for Chemistry **70**, 457 (2016).
- P. Willmott, D. Meister, S. Leake, M. Lange, A. Bergamaschi, M. Böge, M. Calvi, C. Cancellieri, N. Casati, A. Cervellino, Q. Chen, C. David, U. Flechsig, F. Gozzo, B. Henrich, S. Jäggi-Spielmann, B. Jakob, I. Kalichava, P. Karvinen, J. Krempasky, A. Lüdeke, R. Lüscher, S. Maag, C. Quitmann, M. Reinle-Schmitt, T. Schmidt, B. Schmitt, A. Streun, I. Vartiainen, M. Vitins, X. Wang, and R. Wulschleger, Journal of Synchrotron Radiation **20**, 667 (2013).
- A. Bergamaschi, A. Cervellino, R. Dinapoli, F. Gozzo, B. Henrich, I. Johnson, P. Kraft, A. Mozzanica, B. Schmitt, and X. Shi, Journal of Synchrotron Radiation **17**, 653 (2010).
- A. Guinier, G. Fournet, and C. Walker, *Small angle scattering of X-rays* (J. Wiley & Sons: New York, 1955).
- P. Debye, Ann. Physik **46**, 809 (1915).